Robust vibration isolation by frequency-shaped sliding surface control with geophone dynamics

Robust Vibration Isolation by Frequency-Shaped Sliding Surface Control with Geophone Dynamics

Chenyang Ding, A.A.H. Damen, P.P.J. van den Bosch

Abstract— **The Frequency-Shaped Sliding Surface Control (FSSSC) has been recently applied to the Active Vibration Isolation System (AVIS) and the robust skyhook performance is experimentally validated. However, the performance of this approach is theoretically limited by the sensor dynamics. This paper generalizes the FSSSC approach as a two-step AVIS control design method. The first step is to design the sliding surface which determines the designed performances. The second step is to design the regulator which guarantees the convergence of the system dynamics. As long as this convergence is guaranteed, the designed performances would be realized. The vibration isolation of the original plant is therefore transformed to the regulation of a new system which is composed of the original plant and the sliding surface. As the regulator design has been well studied in the literature, this paper focuses on the sliding surface design. An example sliding surface design to achieve low-frequency vibration isolation is provided. The FSSSC of an example 1-DOF plant using both original and the improved sliding surface are compared. Theoretical calculations show that the improved sliding surface has no theoretical performance limit and achieves robust vibration isolation at much lower frequencies than the original design.**

I. Introduction

Many high-precision applications, such as lithographic wafer steppers/scanners used to fabricate integrated circuits or electron microscopes used for sub-micron imaging, demand high performance multiple Degrees Of Freedom (DOF) Active Vibration Isolation Systems (AVIS). The objective of such an AVIS is to support a heavy payload and to reduce the payload vibration which is transmitted from the floor or excited by directly applied force disturbance. The mass of payload is in the order of 10^3 kg. Currently, a 6-DOF AVIS based on three pneumatic isolators [7] is applied in the industry. It compensates the payload gravity by pressurized air. The possibility of contactless AVIS based on three electromagnetic isolators, which compensates the payload gravity by passive Permanent Magnetic (PM) force, is also feasible [8] and being investigated [4], [11]. Active control can be applied to simultaneously achieve stability and vibration isolation on all DOFs. Modal decomposition [5], [7] can be applied to simplify the multi-DOF control problem to 1-DOF control problem. Therefore, a 1-DOF model is used here as an example plant to study the AVIS control.

The objective of the AVIS control is to minimize the payload absolute displacement (the terminology *absolute* indicates that this physical variable is with respect to an inertially fixed reference). The vibration isolation performance is evaluated by the *transmissibility*, defined by the transfer function from the floor vibration to the payload vibration. The disturbance rejection performance is evaluated by *compliance*, defined by the transfer function from the force disturbance to the payload vibration. However, neither floor absolute displacement nor payload absolute displacement is directly measurable by any industrial sensors. Integration of absolute velocity/acceleration signal is not feasible because of the limited performance of the industrial sensors. The following two measurement schemes are widely implemented.

- The relative displacement (payload displacement with respect to the floor) and the payload absolute velocity.
- The relative displacement and the payload absolute acceleration.

Each of them requires a Double-Input-Single-Output (DISO) controller for the 1-DOF AVIS control.

The DISO controller design methods for AVIS has been well studied in the last a few decades. The well-known skyhook control was invented by D. Karnopp [1], [2]. The skyhook performance becomes a standard vibration isolation performance and an excellent reference for some adaptive controls [9]. The skyhook control is based on the assumption that the absolute velocity signal can be perfectly measured. The most widely used industrial velocity sensor is geophone which has its own dynamic characteristics. The geophone sensitivity decreases at low frequencies and reaches zero at zero frequency [5], [12]. Therefore, the low frequency skyhook performance is difficult to achieve by skyhook control. The H_∞ control is applicable to the DISO controller design [3], [4]. By manipulating the weights, the H_∞ control is able to minimize a variable without the direct measurement. It also guarantees robust stability and robust performance. However, the H_∞ control design is usually a iterative process which is quite time-consuming. Besides, the order of the H_∞ controller is usually very high. Order reduction algorithms may apply but the performance would be reduced.

One of the latest achievement on the DISO controller design is provided by L. Zuo and J.J.E. Slotine [5] wherein the Frequency-Shaped Sliding Surface Control (FSSSC) is applied to AVIS control. According to the skyhook transmissibility, a sliding surface is designed based on relative displacement and absolute velocity feedback. The switching control and adaptive control are applied to guarantee that the convergence of the system dynamics despite of unknown disturbances and plant uncertainties. Robust skyhook performance is experimentally validated.

The FSSSC has simple structure and robust performance but the sliding surface design in [5] has a theoretical limit on further lowering the transmissibility resonant frequency due to the velocity sensor dynamics. However, the sensor

978-1-4244-5226-2/10/$26.00 ©2010 IEEE

dynamics could be compensated so that it should not be a theoretical obstacle to improve the transmissibility. It is the sensor noise who destroys the velocity measurement. Therefore, the theoretical limit of lowering the transmissibility resonant frequency could be removed by improving the sliding surface design.

This paper generalizes the FSSSC approach as a two-step AVIS control design method. The first step is to design the sliding surface which determines the designed performances. The second step is to design the regulator which realizes the designed performances. As the regulator design has been well studied in [5], we focus on the sliding surface design. An example sliding surface design which has no theoretical performance limits are provided. The example 1-DOF plant, sensor dynamics, and the AVIS performance requirements are introduced in Section II. Section III introduces the generalized FSSSC approach, including the sliding surface design and the regulator design. The original sliding surface design in [5] and the improved sliding surface design are given in Section IV. FSSSC of the example 1-DOF plant using both sliding surface designs are compared in Section V. This work is concluded in Section VI.

II. Problem Statement

A. 1-DOF Model

A 1-DOF model is introduced as an example plant to study the AVIS control. The physical model of the 1-DOF plant is shown in Fig. 1. The payload mass, spring stiffness, and damping coefficient are denoted by m, k, and c, respectively. For pneumatic isolators, $c > 0$ and $k > 0$. For 1-DOF contactless electromagnetic isolators, $c = 0$ and $k < 0$ (For multi-DOF contactless electromagnetic isolators, there is at least one DOF that has negative stiffness). The payload absolute displacement, payload absolute velocity, and floor absolute displacement are denoted by x_A, v_A, and x_G, respectively. The actuator force is denoted by f_a. The equation of motion for the payload is given by

$$m\ddot{x_A} + c\dot{x_R} + kx_R = f_a, \tag{1}$$

where $x_R = x_A - x_G$ is the relative displacement. The diagram of the physical model is shown in the dashed rectangular in Fig. 2. Define the transfer function P as

$$P(s) = \frac{1}{ms^2}. \tag{2}$$

B. Sensor Models

The signals fedback for control are the payload relative displacement x_R and the payload absolute velocity v_A. The signals $\widetilde{x_R}$ and $\widetilde{v_A}$ are the measured x_R and v_A, respectively. The displacement sensor usually has very high bandwidth (in the order of 10^4 Hz) so that the sensor dynamics is negligible at low frequencies (in the order of 10^2 Hz or lower). The displacement sensor noise, denoted by n_x, is assumed to be independent of x_R so that $\widetilde{x_R}$ is derived by

$$\widetilde{x_R} = x_R + n_x. \tag{3}$$

Geophone is a type of absolute velocity sensor widely used in the industry. The dynamic model [5], [12] for the geophone has the form of

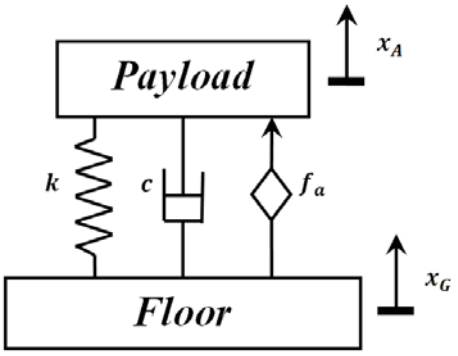

Fig. 1. Physical model of the 1-DOF AVIS.

$$G_v(s) = \frac{s^2}{s^2 + 2\omega_v\xi_v s + \omega_v^2}, \tag{4}$$

where ω_v is the resonant frequency and ξ_v is the damping ratio. The geophone noise, denoted by n_v, is assumed to be independent of v_A. The relation between $\widetilde{v_A}$ and v_A is

$$\widetilde{v_A} = G_v(s)v_A + n_v. \tag{5}$$

C. Performance Requirements

The closed-loop performances are the transmissibility $\mathbb{T}_c$, the compliance $\mathbb{C}_c$, the geophone-noise sensitivity $\mathbb{S}_c$ and the displacement-sensor-noise sensitivity $\mathbb{R}_c$. $\mathbb{S}_c$ and $\mathbb{R}_c$ are concerned because they would affect $|\overline{\mathbb{T}_c}|$, the upper bound of $|\mathbb{T}_c|$. $\mathbb{S}_c$ is defined as the transfer function from the geophone noise to the payload absolute displacement and $\mathbb{R}_c$ is defined as the transfer function from the displacement sensor noise to the payload absolute displacement. The requirements are described as follows.

- $\mathbb{T}_c$, $\mathbb{C}_c$, $\mathbb{R}_c$, and $\mathbb{S}_c$ are all stable.
- Interested frequency range is from zero up to the order of 10^2 Hz.
- $|\mathbb{T}_c(\omega)| = 0$ dB, $\forall\ \omega \in [0, \omega_c]$. $|\mathbb{T}_c(\omega)|$ decreases for all $\omega > \omega_c$ and the decreasing rate is at least -40 dB/dec. ω_c is the cross-over frequency of $\mathbb{T}_c$. Smaller ω_c indicates better transmissibility. Around ω_c, $|\mathbb{T}_c|$ may have a peak. Smaller peak value indicate better transmissibility.
- Low $|\mathbb{C}_c(\omega)|$ for all $\omega \geqslant 0$. Some high performance AVIS require that $|\mathbb{C}_c(0)| = 0$ ($-\infty$ dB).
- $|\mathbb{S}_c(0)| = 0$ ($-\infty$ dB). Low $|\mathbb{S}_c(\omega)|$ for all $\omega > 0$.

III. Generalized FSSSC

The name "frequency-shaped sliding surface" was given by K.D. Young and U. Ozguner [6] in 1993. It is usually applied to tracking control, in which, a measurable signal is to be minimized. It is physically applied to AVIS control by L. Zuo and J.J.E. Slotine [5] in 2004. Therein, the sliding surface is designed for ideal feedback signals. The FSSSC approach is generalized as a two-step AVIS control design method in this section.

The control of the 1-DOF plant P by FSSSC approach is illustrated by the diagram in Fig. 2. The sliding surface is defined by the equation $\sigma = 0$. The blocks Λ_1 and Λ_2 are two transfer functions used to shape the sliding surface. The block R is the regulator. The FSSSC approach can be generalized to a two-step AVIS control design method. The first step is to design the frequency-shaped sliding surface (Λ_1 and Λ_2) which determines the designed performances. The designed sliding surface and the original plant P form a new system P_n, shown as the shaded blocks in Fig. 2. The second step is to design the regulator R for P_n to guarantee the convergence of σ to zero. As long as this convergence is guaranteed, the designed performances can be realized.

A. Sliding Surface Design

The designed performances, which are determined by Λ_1 and Λ_2, are the designed transmissibility $\mathbb{T}_d$, the designed displacement-sensor-noise $\mathbb{R}_d$ and the designed geophone-noise sensitivity $\mathbb{S}_d$. They are defined as

$$\mathbb{T}_d = -\mathbb{R}_d = \frac{\Lambda_1}{\Lambda_1 + \Lambda_2 s G_v},\ \mathbb{S}_d = \frac{-\Lambda_2}{\Lambda_1 + \Lambda_2 s G_v}. \tag{6}$$

According to Fig. 2, the equation $\sigma = 0$ is equivalent to

$$\Lambda_1 \widetilde{x_R} + \Lambda_2 \widetilde{v_A} = 0. \tag{7}$$

Substitute (3) and (5) into (7), we have

$$\Lambda_1 (x_R + n_x) + \Lambda_2 (G_v v_A + n_v) = 0. \tag{8}$$

By applying the Laplace Transform, it can be subsequently used to calculate $|\overline{\mathbb{T}_d}|$, the upper bound of the designed transmissibility magnitude.

$$\frac{X_A}{X_G} = \frac{\Lambda_1}{\Lambda_1 + \Lambda_2 s G_v}\left(1 - \frac{N_x}{X_G}\right) - \frac{\Lambda_2}{\Lambda_1 + \Lambda_2 s G_v}\frac{N_v}{X_G}, \tag{9}$$

where X_A, X_G, N_x, and N_v are Laplace Transform of signals x_A, x_G, n_x, and n_v, respectively. According to (9), $|\overline{\mathbb{T}_d}|$ can be derived as

$$|\mathbb{T}_d| \leqslant |\overline{\mathbb{T}_d}| = |\mathbb{T}_d| + |\mathbb{R}_d|\left|\frac{N_x}{X_G}\right| + |\mathbb{S}_d|\left|\frac{N_v}{X_G}\right|. \tag{10}$$

To make $\mathbb{T}_d$ more robust against the sensor noise, its upper bound has to be reduced. Among all the possible ways to achieve that, reducing $|\mathbb{S}_d|$ is the only way in the field of control design, which relies on the sliding surface design. According to (6), $\mathbb{S}_d$ and $\mathbb{T}_d$ are related by

$$\mathbb{T}_d + s G_v \mathbb{S}_d = 1. \tag{11}$$

Therefore, to simultaneously improve both $\mathbb{S}_d$ and $\mathbb{T}_d$ is impossible with predefined geophone dynamics. The sliding surface design has to make a trade-off between $\mathbb{S}_d$ and $\mathbb{T}_d$.

B. Regulator Design

The objective of the regulator design is to realize the designed performances by keeping $\sigma = 0$. The vibration isolation of the original plant is therefore transformed to the regulation of a new system P_n which is composed of the original plant and the designed sliding surface (Λ_1 and Λ_2). The input is the control force f_a and the output is σ (note that

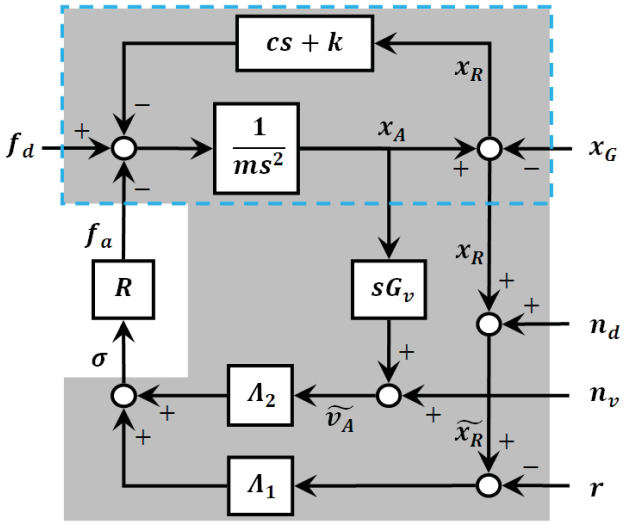

Fig. 2. Generalized FSSSC diagram.

σ is exactly known). The transfer function of P_n is derived according to the shaded blocks in Fig. 2.

$$P_n = (\Lambda_1 + \Lambda_2 s G_v)\frac{1}{ms^2 + cs + k}. \tag{12}$$

The regulator R has to be designed according to the properties of P_n to keep σ zero. If the plant P_n is linear, the regulation can be as simple as PID even if $\mathbb{C}_c(0) = 0$ is required. More advanced methods like optimal control or H_∞ control can also apply. If there exist significant nonlinearity in P_n (due to the original plant), there are also many candidate design methods, for example, back-stepping, sliding mode control, etc.

In [5], the conventional switching control is directly applied as the regulator to reject the unknown disturbances and an adaptive algorithm is proposed to deal with the plant parameter uncertainties. The switching control is described as

$$f_a = -f \cdot \mathrm{sgn}(\sigma), \tag{13}$$

where f is a positive constant. Since the sliding surface is much more complicated than that in [5], directly applied switching control might not be able to stabilize P_n. If that is the case, sliding mode control can be applied to guarantee the convergence of σ to zero under all the unknown disturbances. Boundary layer control can be designed to reduce the chatter. However, boundary layer control rely on linear control design tools [10]. In either cases, switching control or sliding mode control, $\mathbb{T}_d$ and $\mathbb{S}_d$ can be approximately realized.

If the regulator is linear, the FSSSC approach is a linear approach. Based on the linear plant (if it is nonlinear, we assume it can be linearized around a working point), the closed-loop transmissibility $\mathbb{T}_c$ and compliance $\mathbb{C}_c$ can be calculated based on Fig. 2.

$$\mathbb{T}_c = \frac{\Lambda_1 + \frac{cs+k}{R}}{\frac{1}{PR} + \frac{cs+k}{R} + \Lambda_1 + \Lambda_2 s G_v},\ \mathbb{C}_c = \frac{\frac{1}{R}}{\frac{1}{PR} + \frac{cs+k}{R} + \Lambda_1 + \Lambda_2 s G_v}, \tag{14}$$

where $P = \frac{1}{ms^2}$. The closed-loop geophone-noise sensitivity $\mathbb{S}_c$ is calculated as

$$\mathbb{S}_c = \frac{-\Lambda_2}{\frac{1}{PR} + \frac{cs+k}{R} + \Lambda_1 + \Lambda_2 s G_v}. \tag{15}$$

The closed-loop displacement-sensor-noise sensitivity $\mathbb{R}_c$ is calculated as

$$\mathbb{R}_c = \frac{-\Lambda_1}{\frac{1}{PR} + \frac{cs+k}{R} + \Lambda_1 + \Lambda_2 s G_v}. \tag{16}$$

The upper bound of the closed-loop transmissibility magnitude, $|\overline{\mathbb{T}_c}|$, is calculated as

$$|\mathbb{T}_c| \leqslant |\overline{\mathbb{T}_c}| = |\mathbb{T}_c| + |\mathbb{R}_c| \left| \frac{N_x}{X_G} \right| + |\mathbb{S}_c| \left| \frac{N_v}{X_G} \right|. \tag{17}$$

If the open loop gain is so high that the approximations

$$\Lambda_1 + \frac{cs+k}{R} \approx \Lambda_1, \tag{18a}$$

$$\frac{1}{PR} + \frac{cs+k}{R} + \Lambda_1 + \Lambda_2 s G_v \approx \Lambda_1 + \Lambda_2 s G_v, \tag{18b}$$

are feasible, we have $\mathbb{T}_c = \mathbb{T}_d$, $\mathbb{R}_c = \mathbb{R}_d$ and $\mathbb{S}_c = \mathbb{S}_d$. Also, the upper bound in (17) is exactly the same as (10) and $|\mathbb{C}_c|$ is reduced. Therefore, R has to be designed as a high-gain controller to make the approximation (18) feasible. As a result, design of $\mathbb{T}_c$ and $\mathbb{S}_c$ can be accomplished by the sliding surface design. The bottle neck to increase the open-loop gain would be the actuator capacity, the control-loop time-delay, and possible flexible modes.

IV. Example Sliding Surface Design

A. Sliding Surface for Ideal Sensors

Assume that $G_v = 1$, the designed transmissibility $\mathbb{T}_d$ defined in (6) becomes

$$\mathbb{T}_d = \frac{\Lambda_1}{\Lambda_1 + \Lambda_2 s}, \tag{19}$$

In [5], $\Lambda_1 = a_0$ and $\Lambda_2 = a_2 s + a_1$, where $a_i, \forall i \in \{1,2,3\}$ are constants. The designed transmissibility (19) is subsequently derived as

$$\mathbb{T}_d = \frac{a_0}{a_0 + a_1 s + a_2 s^2}, \tag{20}$$

which is exactly the skyhook transmissibility. However, if the geophone dynamics (4) is considered, the actual designed transmissibility can be derived as

$$\mathbb{T}_d = \frac{a_0(s^2 + 2\omega_v \xi_v s + \omega_v^2)}{a_0(s^2 + 2\omega_v \xi_v s + \omega_v^2) + (a_1 + a_2 s)s^3} \tag{21}$$

It is derived in [5] that $\mathbb{T}_d$ in (21) is stable if

$$\frac{\omega_d}{\omega_v} > \frac{\xi_d}{\xi_v} + \frac{\xi_v}{\xi_d}, \tag{22}$$

where ω_d and ω_v are the resonant frequency of $\mathbb{T}_d$ and G_v, respectively. ξ_d and ξ_v are the damping ratio of $\mathbb{T}_d$ and G_v, respectively. A necessary condition to keep $\mathbb{T}_d$ stable is $\omega_d > 2\omega_v$. Ideal skyhook performance can be achieved only if $\omega_d \gg \omega_v$. Therefore, the vibration isolation performance at low frequencies is limited by the sensor dynamics using this sliding surface design.

B. Sliding Surface with Sensor Dynamics

The limit of $\omega_d > 2\omega_v$ can be eliminated by including the geophone dynamics in the sliding surface design. Denote the numerators and denominators of $\Lambda_i, \forall i \in \{1,2\}$ by N_i and D_i, respectively, (6) becomes

$$\mathbb{T}_d = \frac{N_1 D_2 (s^2 + 2\omega_v \xi_v s + \omega_v^2)}{N_1 D_2 (s^2 + 2\omega_v \xi_v s + \omega_v^2) + N_2 D_1 s^3}, \tag{23a}$$

$$\mathbb{S}_d = -\frac{N_2 D_1 (s^2 + 2\omega_v \xi_v s + \omega_v^2)}{N_1 D_2 (s^2 + 2\omega_v \xi_v s + \omega_v^2) + N_2 D_1 s^3}. \tag{23b}$$

Let $D_1 = (s^2 + 2\omega_v \xi_v s + \omega_v^2) D_2$, (23) is simplified to

$$\mathbb{T}_d = \frac{N_1}{N_1 + N_2 s^3}, \qquad \mathbb{S}_d = -\frac{N_2 (s^2 + 2\omega_v \xi_v s + \omega_v^2)}{N_1 + N_2 s^3}. \tag{24}$$

To achieve $\mathbb{S}_d(0) = 0$, the constant term of the polynomial N_2 should be zero. Let $N_2 = N_2' s$, (24) becomes

$$\mathbb{T}_d = \frac{N_1}{N_1 + N_2' s^4}, \qquad \mathbb{S}_d = -\frac{N_2' s (s^2 + 2\omega_v \xi_v s + \omega_v^2)}{N_1 + N_2' s^4}. \tag{25}$$

$\mathbb{T}_d$ can be designed by the choice of N_1 and N_2'. To achieve the -40 dB/dec decreasing rate of $|\mathbb{T}_d|$ at high frequencies, the denominator order should be the numerator order plus two. If the order of $\mathbb{T}_d$ is *four* (this is the lowest), N_2' has to be a constant and the order of N_1 has three possibilities: zero, one or two. In this case, $\mathbb{T}_d$ has the possible forms of $\mathbb{T}_d = \frac{a_0}{a_4 s^4 + a_0}$ or $\mathbb{T}_d = \frac{a_1 s + a_0}{a_4 s^4 + a_1 s + a_0}$ or $\mathbb{T}_d = \frac{a_2 s^2 + a_1 s + a_0}{a_4 s^4 + a_2 s^2 + a_1 s + a_0}$. To make $\mathbb{T}_d$ stable, proper sets of constants $\{a_0, a_4\}$ or $\{a_0, a_1, a_4\}$ or $\{a_0, a_1, a_2, a_4\}$ have to be found, each of which is difficult.

If the order of $\mathbb{T}_d$ is *five*, the two numerators can be designed as $N_1 = a_3 s^3 + a_2 s^2 + a_1 s + a_0$ and $N_2' = a_5 s + a_4$ so that $\mathbb{T}_d$ has the form of

$$\mathbb{T}_d = \frac{a_3 s^3 + a_2 s^2 + a_1 s + a_0}{a_5 s^5 + a_4 s^4 + a_3 s^3 + a_2 s^2 + a_1 s + a_0}. \tag{26}$$

Similarly, the five poles of $\mathbb{T}_d$ can be selected based on criterions of stability and low resonant frequency. Subsequently, the five constants $a_i, \forall i \in \{1,2,3,4,5\}$ are uniquely determined. There are also no theoretical performance limit induced by the geophone resonant frequency. Based on (24), $\mathbb{S}_d$ has the form of

$$\mathbb{S}_d = -\frac{(a_5 s^2 + a_4 s)(s^2 + 2\omega_v \xi_v s + \omega_v^2)}{a_5 s^5 + a_4 s^4 + a_3 s^3 + a_2 s^2 + a_1 s + a_0}. \tag{27}$$

Therefore, both $\mathbb{T}_d$ and $\mathbb{S}_d$ fulfill the design criterions. The design of D_1 and D_2 is to make Λ_1 and Λ_2 stable and to simplify the regulator design. If we continue increasing the order of $\mathbb{T}_d$, higher decreasing rate of $|\mathbb{T}_d|$ or lower $|\mathbb{S}_d|$ can be achieved. The price would be the increased order of the controller.

V. Performance Comparison

If the regulator is linear, the closed-loop transmissibility and its upper bound can be theoretically calculated. The parameters of the geophone dynamics are assumed to be $\omega_v = 2\pi$ rad/s (1 Hz) and $\xi_v = 0.7$ so that the geophone dynamics is calculated as

$$G_v = \frac{s^2}{s^2 + 8.796s + 39.48}. \tag{28}$$

We also assume that $\left|\frac{N_v(\omega)}{X_G(\omega)}\right| = 0.2$ and $\left|\frac{N_x(\omega)}{X_G(\omega)}\right| = 0.1, \forall \omega \geqslant 0$. The example plant with different parameters will be used to test the performance robustness. The model parameters for a pneumatic plant are assumed to be $m = 500$ kg, $c =$ 894 N·s/m, and $k = 10^4$ N/m. The model parameters for an electromagnetic plant are assumed to be $m = 500$ kg, $c = 0$, and $k = -10^4$ N/m.

A. FSSSC Assuming Ideal Sensor

According to (22), ω_d and ξ_d are chosen as $\omega_d = 8\pi$ rad/s (4 Hz) and $\xi_d = 0.7$. The designed sliding surface ignoring the geophone dynamics is

$$\Lambda_1 = \frac{631.7}{s+1}, \qquad \Lambda_2 = \frac{s + 35.19}{s+1}. \tag{29}$$

The designed transmissibility as in (20) is

$$\mathbb{T}_d = \frac{631.7}{s^2 + 35.19s + 631.7}. \tag{30}$$

R is designed as a PID controller.

$$R = \frac{5 \times 10^4 (s^2 + 1.4s + 0.98)}{s}. \tag{31}$$

The designed transmissibility $\mathbb{T}_d$ calculated by (20) and the closed-loop transmissibility $\mathbb{T}_c$ calculated with the geophone dynamics are compared in Fig. 3 for both pneumatic and electromagnetic plants. With different plants, both $\mathbb{T}_d$ and $\mathbb{T}_c$ are almost identical, which indicates that the transmissibility is robust against the plant uncertainties. For each plant, $\mathbb{T}_c$ and $\mathbb{T}_d$ coincide except that $\mathbb{T}_c$ has a resonant peak around 2 Hz, which is caused by the geophone dynamics. $\mathbb{T}_c$ is quite close to its upper bound, which indicates that the closed-loop transmissibility is robust against the sensor noises.

B. FSSSC Considering Geophone Dynamics

Including the geophone dynamics (4) into the sliding surface design, the designed transmissibility $\mathbb{T}_d$ would have higher order. If the order of $\mathbb{T}_d$ is *five*, the five poles of the designed transmissibility are chosen as $[-1.4 + 1.4i, -1.4 - 1.4i, -1.4 + 1.4i, -1.4 - 1.4i, -2]$. The designed sliding surface is

$$\Lambda_1 = \frac{26.88(s + 0.9333)}{s^2 + 8.796s + 39.48}, \; \Lambda_2 = \frac{s^2 + 7.6s}{s^2 + 1.05s + 1.225}. \tag{32}$$

The designed transmissibility is

$$\mathbb{T}_d = \frac{26.88(s + 0.9333)(s^2 + 1.05s + 1.225)}{(s+2)(s^2 + 2.8s + 3.92)^2}. \tag{33}$$

R is designed as a PID controller.

$$R = \frac{5 \times 10^4 (s^2 + 1.4s + 0.98)}{s}. \tag{34}$$

The designed transmissibility $\mathbb{T}_d$ and the closed-loop transmissibility $\mathbb{T}_c$ are compared in Fig. 4 for both pneumatic and electromagnetic plants. With different plants, both $\mathbb{T}_d$ and $\mathbb{T}_c$ are almost identical, which indicates that the vibration isolation performance is robust against the plant uncertainties. For each plant, $\mathbb{T}_c$ and $\mathbb{T}_d$ coincide and they both has the resonant peak. $\mathbb{T}_c$ is reasonably close to its upper bound, which indicates that the transmissibility is robust against the sensor noises at low frequencies. Compared to the closed-loop transmissibility in Fig. 3, the transmissibility resonant frequency is reduced significantly from around 2 Hz to around 0.4 Hz. The high frequency decreasing rate is -40 dB/dec. The robustness against the sensor noise is reduced but acceptable. The overall closed-loop performance is better than the previous design. It can be expected that the sliding surface design could gain more flexibility by increasing the order of the designed transmissibility. The trade-off would be higher controller order.

VI. Conclusion

This paper generalizes the Frequency-Shaped Sliding Surface Control (FSSSC) approach in [5] as a two-step Active Vibration Isolation System (AVIS) control design method, which is applicable to a class of AVIS. The first step is to design the sliding surface based on the dynamics of the relative displacement sensor and absolute velocity sensor (geophone). The objective is make sure that the designed transmissibility and the designed geophone-noise sensitivity fulfill their requirements. The performance limit induced by the geophone dynamics which exists in the original sliding surface design is removed by the improved sliding surface design. It is proved that the transmissibility and the geophone-noise sensitivity can not be improved simultaneously so that a trade-off has to made during the sliding surface design. The second step is the regulator design which is to realize the designed performances. The designed sliding surface and the original plant forms a new system. According to the properties of this new system, the regulator may be nonlinear like sliding mode control or linear like PID. The only design criterion is that the output of this new system converges to zero. Example sliding surface design structures are provided. Based on an example 1-DOF plant, the improved sliding surface design is compared to the original design. Theoretical calculations based on provided parameters show that the improved sliding surface controller realizes vibration isolation at much lower frequency than the original design although the robustness against the sensor noise is slightly reduced. The performance robustness against the plant uncertainties is comparable to the original FSSSC. The future work would be the optimal sliding surface design and the experimental validation.

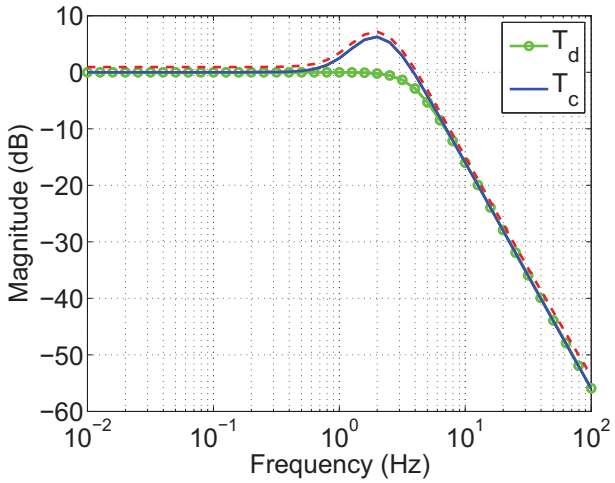

(a) For the pneumatic AVIS.

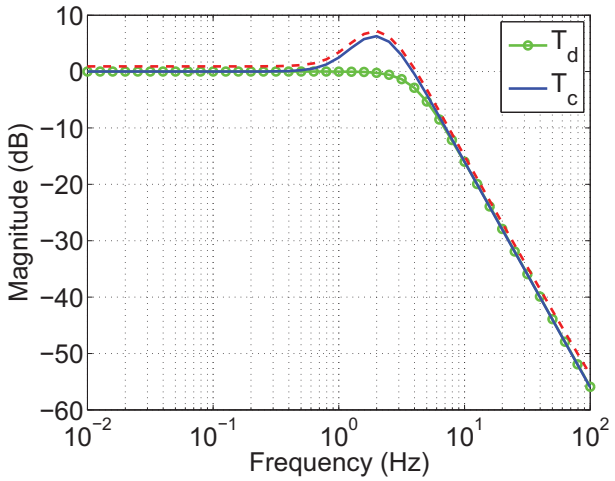

(b) For the electromagnetic AVIS.

Fig. 3. Calculated $|\mathbb{T}_c|$ and $|\mathbb{T}_d|$ according to the original sliding surface design in [5]. The dashed line (red) is the upper bound of $\mathbb{T}_c$ calculated according to (17).

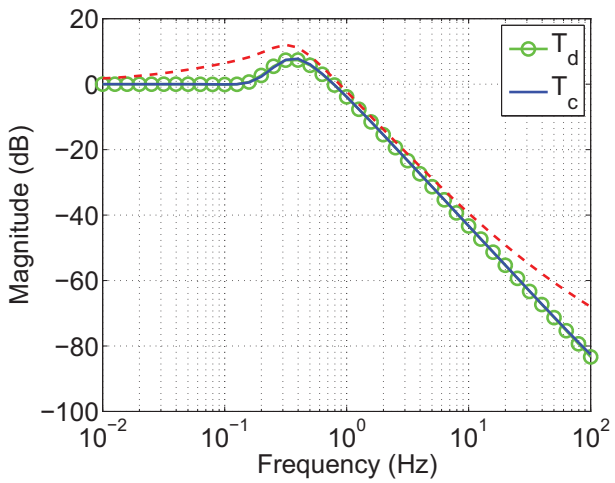

(a) For the pneumatic AVIS.

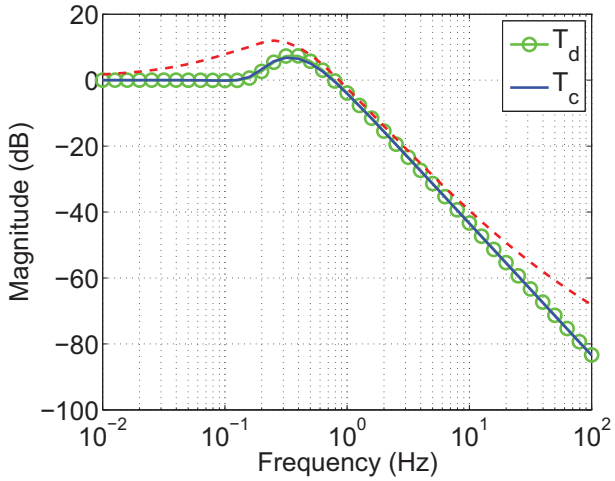

(b) For the electromagnetic AVIS.

Fig. 4. Calculated $|\mathbb{T}_c|$ and $|\mathbb{T}_d|$. $\mathbb{T}_d$ is designed to be 5^{th} order. Geophone dynamics is considered in the designing phase. The dashed line (red) is the upper bound of $\mathbb{T}_c$ calculated according to (17).

VII. ACKNOWLEDGMENTS

This work is a part of the Dutch IOP-EMVT program and is supported financially by SenterNovem, an agency of the Dutch Ministry of Economic Affairs.

REFERENCES

[1] D. Karnopp, M.J. Crosby, and R.A. Harwood, "Vibration Control Using Semi-Active Force Generators", *ASME Journal of Engineering for Industry*, vol. 96, pp. 619-626, 1974.

[2] D. Karnopp, "Active and semi-active vibration isolation", *ASME Journal of Mechanical Design*, vol. 117, pp. 117-185, 1995.

[3] Katsuhide WATANABE, Shinji HARA, Yoichi KANEMITSU, Takahide HAGA, Kenichi YANO, Takayuki MIZUNO, and Ryuta KATAMURA, "Combination of H_∞ and PI Control for an Electromagnetically Levitated Vibration Isolation System", *Proc. 35th Conference on Decision and Control*, Kobe, Japan, Dec. 1996.

[4] C. Ding, A.A.H. Damen, P.P.J. van den Bosch, and J.L.G. Janssen, "Vibration Isolation of an Electromagnetic Actuator with Passive Gravity Compensation", *Proc. 2nd International Conference on Computer and Automation Engineering*, Singapore, Feb. 2010.

[5] L. Zuo and J.J.E. Slotine, "Robust vibration isolation via frequency-shaped sliding control and modal decomposition", *Journal of Sound and Vibration*, vol. 285, no. 4-5, pp.1123-1149, Aug. 2005.

[6] K.D. Young and U. Ozguner, "Frequency shaping compensator design for sliding mode", *International Journal of Control*, vol. 57, no. 5, pp. 1005-1019, 1993.

[7] M. Heertjes, K. de Graaff, and J.G. van der Toorn, "Active Vibration Isolation of Metrology Frames; A Modal Decoupled Control Design", *Journal of Sound and Acoustics-Transactions of the ASME*, vol. 127, Issue 3, pages 223-233, Jun. 2005.

[8] Jeroen L. G. JANSSEN, Johannes J. H. PAULIDES and Elena A. LOMONOVA, "Passive Limitations for a Magnetic Gravity Compensator", *Journal of System Design and Dynamics*, vol. 3, n. 4, pages 671-680, 2009.

[9] L. Zuo, J.J.E. Slotine, S.A. Nayfeh, "Model reaching adaptive control for vibration isolation", *IEEE Trans. on Control Systems Technology*, vol. 13, no. 4, Jul. 2005.

[10] K. D. Young, V.I. Utkin, and U. Ozguner, "A Control Engineer's Guide to Sliding Mode Control", *IEEE Trans. on Control Systems Technology*, vol. 7, no. 3, May 1999.

[11] C. Ding, J.L.G. Janssen, A.A.H. Damen, and P.P.J. van den Bosch, "Modeling and Control of a 6-DOF Contactless Electromagnetic Suspension System with Passive Gravity Compensation", *Proc. XIX International Conference on Electrical Machines*, Rome, Italy, Sep. 2010.

[12] Jinpyo Honga and Kyihwan Park, "Design and control of six degree-of-freedom active vibration isolation table", *Review of Scientific Instruments*, vol 81, issue 3, 2010.